Local structure of the SnTe topological crystalline insulator: Rhombohedral distortions emerging from the rocksalt phase

K. V. Mitrofanov
Nanoelectronics Research Institute, National Institute of Advanced Industrial Science and Technology (AIST), 1-1-1 Higashi, Tsukuba, Ibaraki 305-8562, Japan

A. V. Kolobov* and P. Fons
Nanoelectronics Research Institute & Green Nanoelectronics Center, National Institute of Advanced Industrial Science and Technology (AIST), 1-1-1 Higashi, Tsukuba, Ibaraki 305-8562, Japan and Japan Synchrotron Radiation Research Institute (JASRI), SPring-8, Mikazuki, Hyogo 679-5198, Japan

M. Krbal
Faculty of Chemical Technology, Department of General and Inorganic Chemistry, University of Pardubice, Legion's square 565, 530 02 Pardubice, Czech Republic

T. Shintani
Green Nanoelectronics Center, National Institute of Advanced Industrial Science and Technology (AIST), West 7A, Onogawa 16-1, Tsukuba, Ibaraki 305-8569, Japan

J. Tominaga
Nanoelectronics Research Institute & Green Nanoelectronics Center, National Institute of Advanced Industrial Science and Technology (AIST), 1-1-1 Higashi, Tsukuba, Ibaraki 305-8562, Japan

T. Uruga
Japan Synchrotron Radiation Research Institute (JASRI), SPring-8, Mikazuki, Hyogo 679-5198, Japan

(Received 23 February 2014; revised manuscript received 15 September 2014; published 6 October 2014)

$A^{IV}B^{VI}$ crystals are believed to possess a rhombohedral (ferroelectric) structure at low temperature that changes to the rocksalt (paraelectric) structure above the Curie temperature. For GeTe it has been recently demonstrated that locally the structure retains the subsets of the shorter and longer bonds across the ferroelectric-to-paraelectric transition despite acquiring the cubic structure on average. Nothing is known about the existence of local distortions in SnTe, a prototypical topological crystalline insulator, where the crystal symmetry plays a crucial role. In this work we report the results of x-ray absorption measurements. We find that the structure is locally rhombohedrally distorted, and the distortions increase at $T > 100$ K, breaking the rocksalt average symmetry. Our density functional theory simulations performed at 0 K indicate that the role of spin-orbit coupling in the formation of the local structure of SnTe at low temperature is negligibly small. The small stochastic distortions do not affect the intrinsic band inversion of SnTe.

DOI: 10.1103/PhysRevB.90.134101 PACS number(s): 61.05.cj, 71.15.Mb

I. INTRODUCTION

$A^{IV}B^{VI}$ narrow-gap semiconductors, of which GeTe, SnTe, and PbTe are representatives, are the simplest conceivable class of ferroelectrics with only two atoms in the primitive cell. Based on (mainly) diffraction studies, ferroelectric transitions in these materials were reported when the structure changed from rhombohedral at low temperature to rocksalt at higher temperatures. The transition was determined to be displacive in nature. The Curie temperature for GeTe is about 670 K, while for SnTe it is much lower, with ca. 100 K being the carrier-free limit [1]. The reported experimental values are usually much lower. For PbTe, extrapolation of the experimental data yields a Curie point of −79 K [2], i.e., the latter is always a paraelectric. Discussions of ferroelectric properties of these materials, mainly GeTe, are typically limited to structural studies as the high conductivity in these materials "in all probability prevents switching of orientational states by an external electric field for these systems" [1]. The structure of these materials has been intensively studied by various groups and the origin of the rhombohedral distortions is usually described in terms of the competing covalent and ionic nature of bonding or resonant bonds [3–8].

At present, interest in these materials has been renewed due to the use of GeTe-based alloys in phase-change memory [9] and a possible Rashba splitting in the bulk phase [10] with implications for spintronics applications. PbTe is one of the best thermoelectric materials for applications at and above room temperature. The low thermal conductivity in PbTe was recently attributed to giant anharmonic phonon scattering due to longitudinal acoustic-transverse optic coupling near a lattice instability of the ferroelectric type [11]. SnTe, on the other hand, represents a class of materials known as topological crystalline insulators [12,13]. In the latter, the robust surface states with four dissipationless Dirac cones are

*a.kolobov@aist.go.jp

topologically protected by the mirror symmetry of the crystal rather than time-reversal symmetry. All theoretical arguments are based on the fact that the structure of SnTe has rocksalt symmetry. The topological properties of SnTe have also been confirmed experimentally and some interesting ideas for practical applications have been suggested, e.g., a topological transistor device, in which charge and spin transport are maximally entangled and simultaneously controlled by an electric field [14].

It is now time to note that recent findings based on local structural studies using x-ray absorption spectroscopy [15] and total scattering [16] revealed that GeTe retains rhombohedral distortions at temperatures well above the Curie temperature. The inconsistency between the earlier Bragg diffraction results and subsequent local structure experiments is due to the fact that Bragg diffraction probes the spatially average structure and cannot "see" stochastic local distortions [17,18]. As a result, when the coherency in the direction of the rhombohedral distortions is lost at elevated temperatures, the structure becomes cubic on average, but remains rhombohedrally distorted locally. The transition was consequently re-determined to be an order-disorder transition [15]. Subsequent experiments provided further support for this description [19].

These results suggest that the homologous SnTe compound may also be rhombohedrally distorted locally giving rise to the following questions. Is the structure of SnTe really rocksalt? How does the local structure change with temperature? If the structure of SnTe is indeed perfect rocksalt, what determines the difference between GeTe and SnTe local structures? To address these issues, we have performed extended x-ray absorption fine structure (EXAFS) measurements and *ab-initio* computer simulations, the details of which are described below. EXAFS is a local probe with the characteristic measurement time of ca. 10^{-15} s and thus is capable of taking a true snapshot of the local structure.

II. EXPERIMENTAL AND SIMULATIONS DETAILS

Samples for the experiment were 2 μm-thick films deposited on both sides of a 15 μm-thick Al foil using rf sputtering. X-ray diffraction measurements confirmed that the deposited films were crystalline and possessed an average rocksalt structure. The foil was subsequently cut into 1×1 cm pieces and stacked to optimize the edge jump at both the Sn and Te K edges. EXAFS measurements were performed at beam line BL01B1 at SPring-8 in transmission mode over a temperature range from 10 K to room temperature. For maximum reliability, data measured at both edges were fitted simultaneously.

The density functional calculations were carried out using the VASP code (Vienna *Ab-Initio* Simulation Package) using a $12\times12\times12$ Monkhorst-Pack grid [20]. Projector augmented pseudopotentials (PAW) were used as a basis with a cutoff energy of 250 eV [21]. The PAWs included the valence atomic configuration $5s^25p^4$ for Te and $5s^25p^2$ for Sn with the remainder of the electrons being treated as core electrons. The Perdew-Burke-Ernzerhof generalized gradient approximation (GGA-PBE) was used for the density functional [22]. The calculation was carried out both with and without self-consistent spin-orbit coupling corrections as indicated in the text. For all calculations, the lattice was allowed to relax within the rhombohedral space group with an electronic convergence criteria of 10^{-5} eV and an ionic relaxation loop criteria of 10^{-4} eV.

III. RESULTS AND DISCUSSION

Figure 1 shows the raw EXAFS oscillations for the Te K edge and the corresponding Fourier-transformed spectra for measurements taken at different temperatures. The presence of well defined peaks up to 10 Å indicates the very high quality of the experimental data. Already a visual examination of the spectra allows one to make several interesting observations. First, the raw EXAFS oscillations damp abruptly at $T \approx 100$ K. Second, it is interesting to note that the peaks in the Fourier transformed spectra decrease at a comparable pace for both the nearest neighbors and further shells. This behavior is not typical for solids because of the correlated dynamics of nearest-neighbor atoms [23]. It is interesting to note that a similar behavior was observed for PbTe when an alternative local-structure probe, namely, total scattering with subsequent pair-distribution function (PDF) analysis was used [24]. It is also informative to note that the relative intensities of the

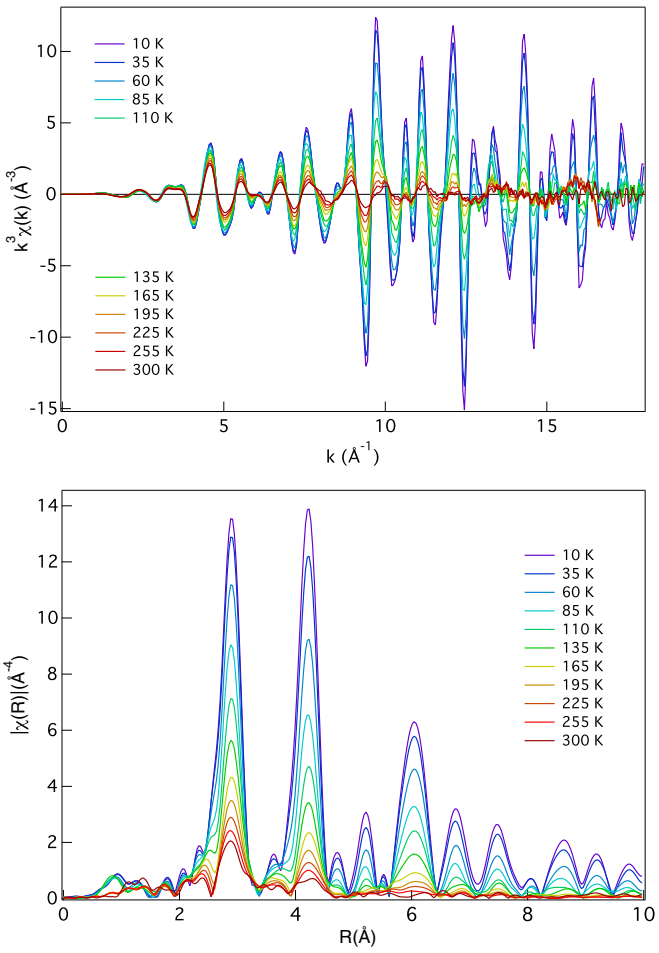

FIG. 1. (Color online) Raw EXAFS oscillations of SnTe measured at Te K edge (top) and the corresponding k^3-weighted Fourier transformed spectra (bottom). The corresponding temperatures are marked in the figure.

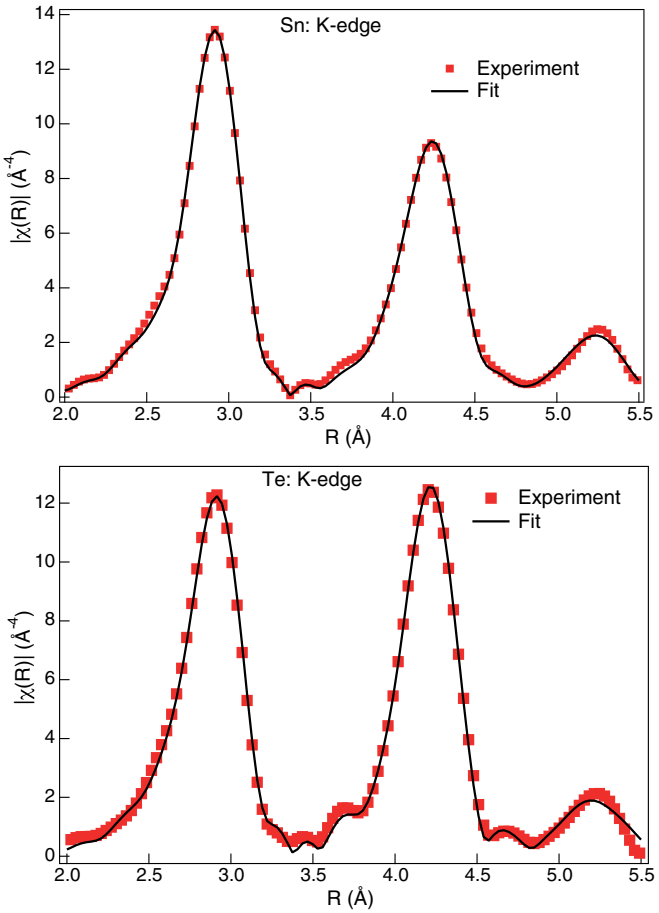

FIG. 2. (Color online) Experimental (10 K) and simulated results (k^3 weighted) for the Sn and Te edges.

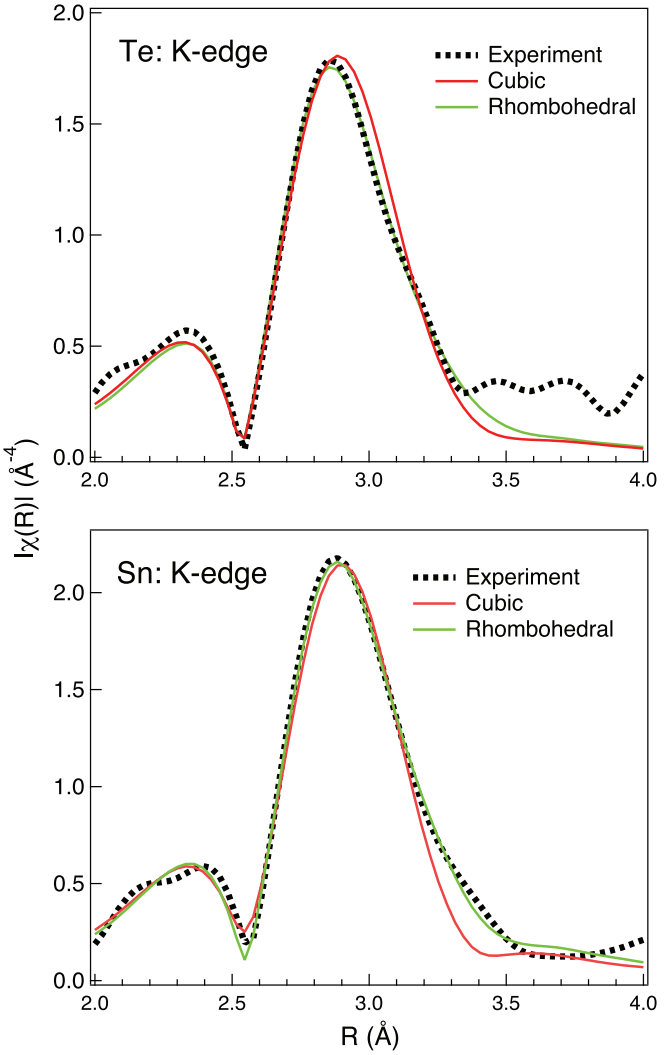

FIG. 3. (Color online) R space fitting of the Te and Sn K edges at room temperature using the rhombohedral and cubic models.

first and second shells (Fig. 2) are different depending upon whether Sn or Te is the central (i.e., absorbing) atom. Since the backscattering amplitudes of Sn and Te are rather similar and the rocksalt structure suggests that the local geometries around the two species are identical, one would expect very similar EXAFS spectra. The fact that the second-nearest neighbor peak is stronger is an indication that the Te sublattice is more ordered. The situation is very similar to the case of $Ge_2Sb_2Te_5$, where the second peak is quite strong for the Te edge and almost invisible for the Ge edge [25,26].

While an apparently good quality fit can be obtained up to the third shell (Fig. 2), inclusion of the higher shells in the fitting aiming at finding local distortions is not productive. Indeed, one can only productively use higher shells when the distortions are coherent. On the other hand, when the (small) local distortions are stochastic, one cannot build a unique model beyond the first-nearest neighbors and, importantly, the tendency of the structure to become cubic on average will result in the higher shells being better fitted by the cubic model, masking the local distortions in the way similar to the Bragg diffraction. To avoid this, the local structure was analyzed using the fitting for the first shell only. In the fitting process, we tried both the perfect rocksalt and a rhombohedrally distorted structure. In the former, the coordination number was fixed at 6, while in the latter a 3 + 3 coordination was assumed. The fit quality was better for the rhombohedrally distorted structure (e.g., at room temperature reduced $\chi^2 = 9.76$ for the cubic phase vs reduced $\chi^2 = 2.76$ for the distorted phase). As an example, in Fig. 3 we show the fitting results at room temperature at both Te and Sn K edges in R space.

The fitting results using the rhombohedral model are shown in Fig. 4, where the temperature dependencies for the shorter and longer Sn-Te bonds are shown. Other fitting parameters included mean-square relative displacements for the shorter and longer bonds and the corresponding energy corrections E_0. One can see that locally the structure of SnTe is distorted; the distortion is essentially constant at $T < 100$ K and then starts to increase. It is also interesting to note that a very asymmetric local structure with the shorter and longer Sn-Te bonds of 2.97 and 3.18 Å was observed when Sn atoms were incorporated into an isoelectronic structure of GeTe [27]. The authors attributed this result to the existence of s^2 lone-pair electrons that become stereochemically active in the alloy.

In Fig. 5 we show the temperature dependence of the mean-square relative displacement (MSRD), which includes both static and dynamic components, the latter being due to thermal

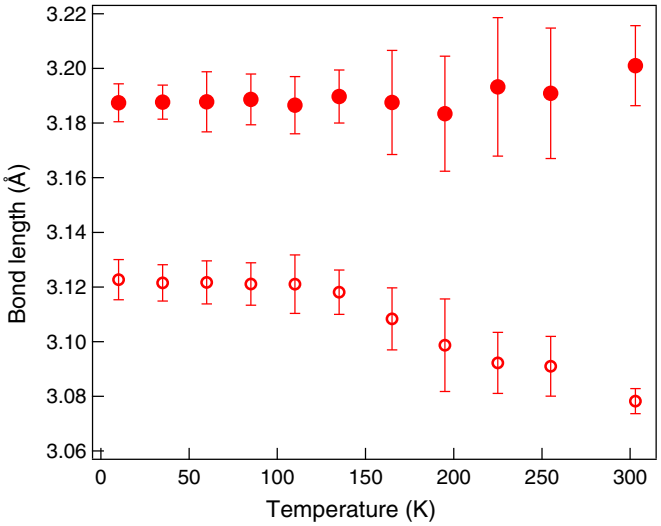

FIG. 4. (Color online) Temperature dependence of the shorter (open circles) and longer (closed circles) Sn-Te bond lengths. The k range using fitting was 15 $Å^{-1}$ for all temperatures.

vibrations and its magnitude determines the rigidity of the bond. The extent to which the MSRD increases with temperature as well as its absolute value are determined by the bond strength usually represented by an Einstein temperature Θ_E that is related to the MSRD σ through the following equation:

$$\sigma^2 = \frac{\hbar^2}{2\mu k_B \Theta_E} \coth\left(\frac{\Theta_E}{2T}\right) + \sigma_0^2. \quad (1)$$

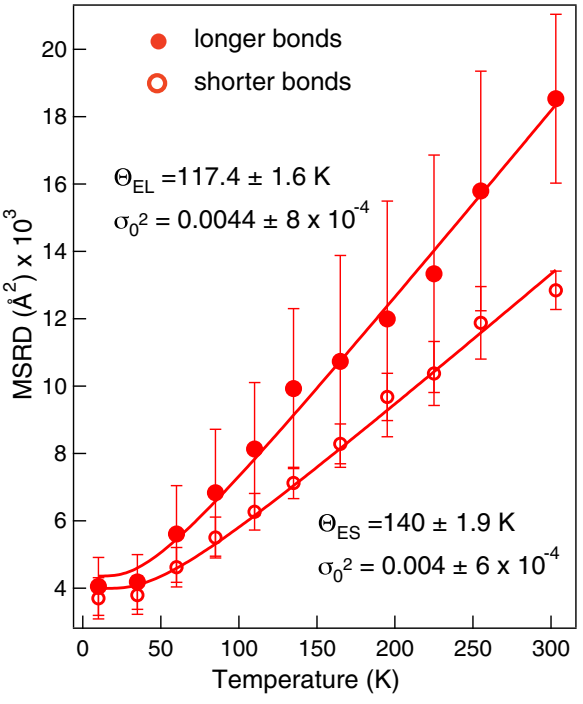

FIG. 5. (Color online) Temperature dependence of mean-square relative displacement for the shorter (open circles) and longer (closed circles) Sn-Te bonds. The fitting yields values of $\Theta_{ES} = 140$ K for the shorter and $\Theta_{EL} = 117$ K for the longer Sn-Te bonds.

Here, μ is the reduced mass, k_B is Boltzmann's constant, and σ_0 is static disorder. The Einstein temperature is typically around 300 K for tetrahedrally bonded semiconductors, around 120–150 K for Se and Te that form helical chains with only two first-nearest neighbors, and in a 30 to 60 K range for clathrates. The fitting of the experimental data yields a value of ca. 140 K for the shorter and ca. 120 K for the longer SnTe bonds, demonstrating that bonds in SnTe are rather soft, as expected for resonant bonding, and in agreement with the findings of [24,28]. For comparison, the homologous GeTe compound has a higher Einstein temperature of 180 K for the shorter bonds.

The experimentally observed much smaller values of local distortions in SnTe compared to GeTe may be associated with a stronger spin-orbit coupling in SnTe. Indeed, it has been argued that the main driving force for the more symmetric Po structure (simple cubic) as opposed to twofold coordinated Te chains with four longer interchain bonds is the stronger spin-orbit coupling [29,30]. The authors have also used different values of spin-orbit coupling to simulate the hypothetical structure of Te and found that stronger spin-orbit coupling led to a smaller Peierls distortion of the structure. To verify the applicability of this hypothesis, we have performed structural relaxation of GeTe and SnTe (using the $R3M$ space group) with and without spin-orbit coupling included in the simulations.

For GeTe, the structural relaxation at 0 K with/without spin-orbit coupling yielded the shorter and longer bond lengths of 2.86 Å/3.22 Å and 2.83 Å/3.32 Å, respectively, with the ratio of the longer/shorter distances being 1.13 with spin-orbit coupling vs 1.17 without. One can see that the inclusion of spin-orbit coupling results in a more symmetric (more cubic) structure. For SnTe, on the other hand, the simulated structure is essentially cubic even without the inclusion of spin-orbit coupling ($R_{\text{short}} = 3.2009$ vs $R_{\text{long}} = 3.2023$ Å). Inclusion of spin-orbit coupling does increase the symmetry ($R_{\text{short}} = 3.2015$ vs $R_{\text{long}} = 3.2030$ Å) but the effect of spin-orbit coupling is negligibly small. We thus conclude that the more symmetric local structure of SnTe, as opposed to GeTe, is due to the larger nuclear charge of Sn and hence to a smaller degree of sp hybridization, resulting in a more "cubic" structure. While it requires further study, it may also be speculated that the difference in the effect of spin-orbit coupling between the Po and SnTe cases is that the resonant bonds in Po are three-center four electron bonds [31], while in SnTe they are three-center two-electron bonds [8].

The observed temperature variation of the bond length is even more intriguing. A nonincreasing bond-length with temperature has been previously observed in resonantly bonded GeTe and Ge-Sb-Te alloys. In particular, in the binary GeTe with increasing temperature the shorter bond remains essentially unchanged [15] while it becomes shorter in $Ge_2Sb_2Te_5$ [8,32]. The origin of the rhombohedral distortion in these materials is usually attributed to a Peierls instability, in which case one would expect a decrease in the distortion with temperature since the thermal population of the conduction band as a consequence of the narrow gap makes the distortion energetically unfavorable, which is the opposite to what is observed experimentally. It may be that in resonantly bonded solids, where the longer bonds are formed using the back lobes of the orbitals that serve to form the shorter (stronger) bonds, an intrinsic

bonding energy hierarchy is present [8]. The weaker bonds are more sensitive to the atomic (mis)alignment [6,8] and weaken further upon increased amplitude of thermal vibrations.

It is interesting that recently a similar behavior, i.e., the emergence of distortions at higher temperatures, was observed for PbTe [24]. An explanation was offered in terms of thermodynamic arguments. It was concluded that the structure of PbTe is the ideal rocksalt at low temperatures but local rhombohedral distortions emerge at temperatures above ca. 150 K giving rise to the formation of randomly oriented local dipoles in the overall paraelectric phase. It was also found that the locally distorted structure possessed a larger band gap [24].

The observation of emerging local dipoles in PbTe triggered a number of subsequent studies that yielded controversial results. Thus a study using charge density visualization using synchrotron powder x-ray diffraction data analyzed with the maximum entropy method [33] suggested very large off-center displacements for Pb (0.25 Å at 105 K and 0.3 Å at 300 K) in agreement with the findings of [24].

The effect was further studied in [28] using *ab-initio* simulations. The authors confirmed the large anharmonicity of PbTe but the formation of local dipoles was not reproduced up to room temperature. It should also be noted that subsequent experimental studies of the temperature dependence of the local structure of PbTe using EXAFS [34] were in disagreement with the conclusions of [24]. In particular, it was argued that the fitting of the experimental EXAFS data using the third cumulant yields a structure without any noticeable Pb atom off-centering, leaving open the question of the formation of local dipoles in PbTe at elevated temperatures. It is not clear why the total scattering and EXAFS data analyses yielded different results for PbTe since their previous use for GeTe demonstrated a very good agreement between the two techniques [16].

We believe that the increasing (or emerging) local rhombohedral distortions (local dipoles) may be a general phenomenon characteristic of resonantly bonded solids. This effect is of particular importance for the topological properties of SnTe, since the gap opening due to temperature-induced local distortions may destroy the Dirac states and intrinsically limit applications of the topological properties of SnTe material to low temperatures.

To address the effect of the stochastic local distortions on the topological properties of SnTe, we performed band structure calculations for the ideal rocksalt and rhombohedrally distorted phases; for the latter we used the experimental values of the shorter and longer Sn-Te bonds obtained from an EXAFS analysis. In Fig. 6 (upper panel) we show the Brillouin zones for the rocksalt phase (left) and for the rhombohedrally distorted phase (right) with the corresponding k points marked. As the structure becomes rhombohedrally distorted, hexagonal planes in the Brillouin zones split into two groups, with the k points corresponding to the centers of the hexagons usually referred to as L and Z. For the cubic phase the L and Z points are obviously equivalent. In the rocksalt phase of SnTe, band inversion has been confirmed at the L point, as evidenced by the larger size of the circles, depicting the contribution of the Te *p* states, at the bottom of the conduction band compared to the top of the valence band (Fig. 6, left). This result is in perfect agreement with previous simulations by others [12] and, in particular, the larger weighting of Te *p* orbitals in

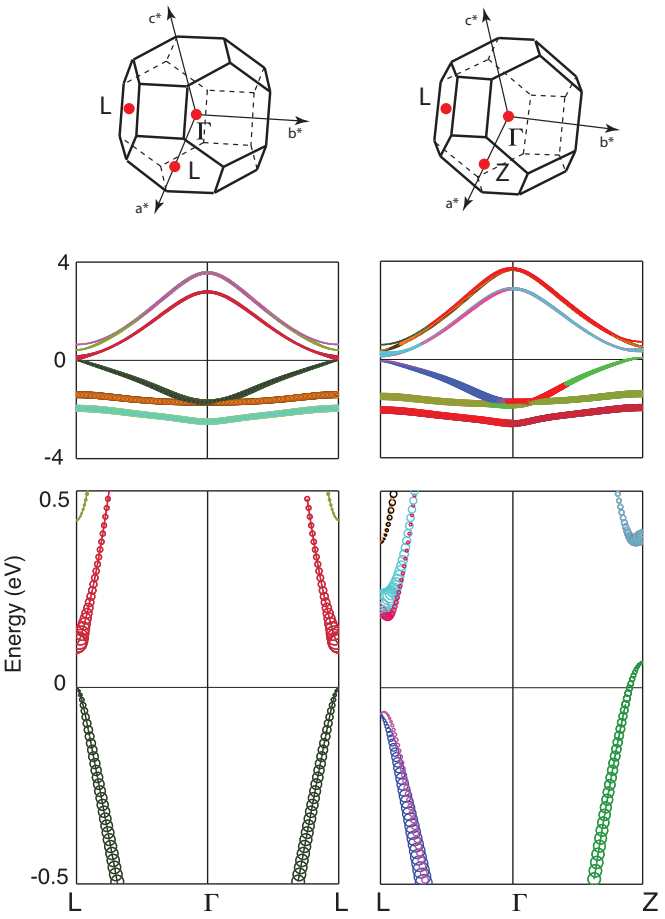

FIG. 6. (Color online) Upper panel: Brillouin zones; middle and lower panels: band structures shown with different energy scales for the ideal rocksalt phase (left) and the rhombohedrally distorted phase (right) of SnTe. The size of the circles corresponds to the weighting of Te *p* orbitals in the shown bands. The larger circles at the bottom of the conduction band compared to the top of the valence band are indicative of band inversion at the L (and Z) point.

the conduction band compared to that of the valence band indicates the intrinsic band inversion at the L point [12]. The band structure for the rhombohedrally distorted phase is shown in Fig. 6 (right). While the overall shape is rather similar, the band structure of the rhombohedrally distorted phase has more bands. More importantly, the band structure changes from direct to indirect but the band inversion is not effected by the emerging rhombohedral distortions (Fig. 6, lower right panel) suggesting that the average symmetry may be more important than local symmetry.

In conclusion, our EXAFS measurements demonstrate that the structure of SnTe is locally distorted and, as the temperature increases, the stochastic rhombodedral distortions increase. We argue that this behavior may be typical of solids with resonant bonding. The stochastic local distortions do not have a strong effect on the intrinsic band inversion of SnTe.

ACKNOWLEDGMENTS

EXAFS measurements were performed within the 2013B1271 project approved by SPring-8. M.K. acknowledges

the project CZ.1.07/2.3.00/20.0254 "ReAdMat—Research Team for Advanced Non Crystalline Materials" cofinanced by the European Social Fund and the state budget of the Czech Republic

[1] M. E. Lines and A. M. Glass, *Principles and Applications of Ferroelectrics and Related Materials* (Clarendon Press, Oxford, 2001).
[2] R. Bate, D. Carter, and J. Wrobel, Phys. Rev. Lett. **25**, 159 (1970).
[3] *Physics of Ferroelectrics: A Modern Perspective*, edited by K. M. Rabe, C. H. Ahn, and J.-M. Triscone, Topics in Applied Physics Vol. 105 (Springer, Berlin, 2007).
[4] K. M. Rabe and J. D. Joannopoulos, Phys. Rev. B **36**, 6631 (1987).
[5] U. V. Waghmare, N. Spaldin, H. C. Kandpal, and R. Seshadri, Phys. Rev. B **67**, 125111 (2003).
[6] G. Lucovsky and R. White, Phys. Rev. B **8**, 660 (1973).
[7] K. Shportko, S. Kremers, M. Woda, D. Lencer, J. Robertson, and M. Wuttig, Nat. Mater. **7**, 653 (2008).
[8] A. V. Kolobov, M. Krbal, P. Fons, J. Tominaga, and T. Uruga, Nat. Chem. **3**, 311 (2011).
[9] A. V. Kolobov and J. Tominaga, *Chalcogenides: Metastability and Phase Change Phenomena* (Springer, Heidelberg, 2012).
[10] D. Di Sante, P. Barone, R. Bertacco, and S. Picozzi, Adv. Mater. **25**, 509 (2013).
[11] O. Delaire, J. Ma, K. Marty, A. F. May, M. A. McGuire, M.-H. Du, D. J. Singh, A. Podlesnyak, G. Ehlers, M. Lumsden *et al.*, Nat. Mater. **10**, 614 (2011).
[12] T. H. Hsieh, H. Lin, J. Liu, W. Duan, A. Bansil, and L. Fu, Nat. Commun. **3**, 982 (2012).
[13] Y. Tanaka, Z. Ren, T. Sato, K. Nakayama, S. Souma, T. Takahashi, K. Segawa, and Y. Ando, Nat. Phys. **8**, 800 (2012).
[14] J. Liu, T. H. Hsieh, P. Wei, W. Duan, J. Moodera, and L. Fu, Nat. Mater. **13**, 178 (2014).
[15] P. Fons, A. V. Kolobov, M. Krbal, J. Tominaga, K. S. Andrikopoulos, S. N. Yannopoulos, G. A. Voyiatzis, and T. Uruga, Phys. Rev. B **82**, 155209 (2010).
[16] T. Matsunaga, P. Fons, A. V. Kolobov, J. Tominaga, and N. Yamada, Appl. Phys. Lett. **99**, 231907 (2011).
[17] E. Stern and Y. Yacoby, J. Phys. Chem. Solids **57**, 1449 (1996).
[18] T. Egami and S. J. L. Billinge, *Underneath the Bragg Peaks: Structural Analysis of Complex Materials* (Pergamon, Oxford, 2003).
[19] F. Kadlec, C. Kadlec, P. Kužel, and J. Petzelt, Phys. Rev. B **84**, 205209 (2011).
[20] G. Kresse and J. Furthmuller, Comp. Mater. Sci. **6**, 15 (1996).
[21] G. Kresse and D. Joubert, Phys. Rev. B **59**, 1758 (1999).
[22] J. P. Perdew, K. Burke, and M. Ernzerhof, Phys. Rev. Lett. **77**, 3865 (1996).
[23] I.-K. Jeong, T. Proffen, F. Mohiuddin-Jacobs, and S. J. Billinge, J. Phys. Chem. A **103**, 921 (1999).
[24] E. S. Božin, C. D. Malliakas, P. Souvatzis, T. Proffen, N. A. Spaldin, M. G. Kanatzidis, and S. J. Billinge, Science **330**, 1660 (2010).
[25] A. Kolobov, P. Fons, A. Frenkel, A. Ankudinov, J. Tominaga, and T. Uruga, Nat. Mater. **3**, 703 (2004).
[26] M. Krbal, A. V. Kolobov, P. Fons, J. Tominaga, S. R. Elliott, J. Hegedus, A. Giussani, K. Perumal, R. Calarco, T. Matsunaga *et al.*, Phys. Rev. B **86**, 045212 (2012).
[27] A. I. Lebedev, I. A. Sluchinskaya, V. N. Demin, and I. H. Munro, Phys. Rev. B **55**, 14770 (1997).
[28] Y. Zhang, X. Ke, P. R. C. Kent, J. Yang, and C. Chen, Phys. Rev. Lett. **107**, 175503 (2011).
[29] B. I. Min, J. H. Shim, M. S. Park, K. Kim, S. K. Kwon, and S. J. Youn, Phys. Rev. B **73**, 132102 (2006).
[30] C.-J. Kang, K. Kim, and B. I. Min, Phys. Rev. B **86**, 054115 (2012).
[31] A. V. Kolobov, P. Fons, J. Tominaga, and S. R. Ovshinsky, Phys. Rev. B **87**, 165206 (2013).
[32] T. Matsunaga, N. Yamada, R. Kojima, S. Shamoto, M. Sato, H. Tanida, T. Uruga, S. Kohara, M. Takata, P. Zalden *et al.*, Adv. Funct. Mater. **21**, 2232 (2011).
[33] S. Kastbjerg, N. Bindzus, M. Søndergaard, S. Johnsen, N. Lock, M. Christensen, M. Takata, M. A. Spackman, and B. B. Iversen, Adv. Funct. Mater. **23**, 5477 (2013).
[34] T. Keiber, F. Bridges, and B. C. Sales, Phys. Rev. Lett. **111**, 095504 (2013).